ISSN 0023-1584, Kinetics and Catalysis, 2011, Vol. 52, No. 6, pp. 855–861. © Pleiades Publishing, Ltd., 2011.
Original Russian Text © D.V. Demidov, I.P. Prosvirin, A.M. Sorokin, T. Rocha, A. Knop-Gericke, V.I. Bukhtiyarov, 2011, published in Kinetika i Kataliz, 2011, Vol. 52, No. 6, pp. 877–883.

Preparation of Ag/HOPG Model Catalysts with a Variable Particle Size and an In Situ XPS Study of Their Catalytic Properties in Ethylene Oxidation

D. V. Demidov[a], I. P. Prosvirin[a], A. M. Sorokin[a], T. Rocha[b], A. Knop-Gericke[b], and V. I. Bukhtiyarov[a]

[a] *Boreskov Institute of Catalysis, Siberian Branch, Russian Academy of Sciences, Novosibirsk, 630090 Russia*
[b] *Fritz-Haber-Institut der Max-Planck-Gesellschaft, Berlin, Germany*
e-mail: demidoff@catalysis.ru

Received May 17, 2011

Abstract—The preparation of model silver catalysts supported on highly oriented pyrolytic graphite is described, and the effect of the Ag particle size on the catalytic ethylene oxidation into ethylene oxide, studied by in situ XPS and mass spectrometry, is considered. For a mean particle diameter of 8 nm, the adsorbed oxygen species characterized by an O 1*s* binding energy of 530.8 ± 0.2 eV (electrophilic oxygen) forms on the silver surface exposed to the ethylene–oxygen reaction mixture. Larger silver particles with a mean diameter of 40 nm additionally contain the adsorbed oxygen species characterized by an O 1*s* binding energy of 529.2 ± 0.2 eV (nucleophilic oxygen). The presence of both oxygen species on the surface of the larger particles ensures the formation of ethylene oxide, while the sample with the smaller silver particles is inactive in the epoxidation reaction. The O 1*s* signal at 530.8 eV is partly due to oxygen dissolved in the subsurface layers of silver.

DOI: 10.1134/S002315841106005X

In recent years, there has been increasing interest in the preparation and study of nanosized metal catalysts in view of the fact that the physical and chemical properties of these catalysts and, accordingly, their catalytic activity depend strongly on their particle size in the nanometer range [1, 2]. There are data indicating the size dependence of the catalytic activity of silver in some reactions. For example, propylene oxidation and low-temperature CO oxidation take place on silver particles no larger than 5 nm [3, 4], while ethylene epoxidation involves Ag particles at least 30 nm in size [5, 6]. The latter reaction—ethylene oxidation into ethylene oxide over $Ag/\alpha\text{-}Al_2O_3$ catalysts—has been implemented in industry on a large scale. Investigation of this reaction on model catalysts demonstrated that it involves two oxygen species adsorbed on silver, namely, "nucleophilic" oxygen O_{nucl} (O 1*s* binding energy of BE = 528.3 eV) and "electrophilic" oxygen O_{el} (BE = 530.5 eV) [7]. The role of nucleophilic oxygen in ethylene epoxidation is to generate olefin adsorption sites (Ag^+). At the same time, this oxygen species can oxidize ethylene to CO_2 and H_2O. Electrophilic oxygen participates in selective ethylene oxidation to ethylene oxide [8–10].

Investigation of size effects on real porous catalysts by surface-sensitive methods is sometimes impossible because of the low surface concentration of the active component. In addition, the spectral characteristics of reaction intermediates adsorbed on the surface are often masked by signals from functional groups of the support. For example, the intense photoelectron peak of oxygen contained in Al_2O_3 totally overlaps the weaker peak from the oxygen species bound to silver, although these peaks differ in binding energy. This problem can be solved by using model catalytic systems such as active metal particles supported on highly oriented pyrolytic graphite (HOPG) [11–15]. The absence of oxygen in HOPG makes it possible to successfully use surface-sensitive methods, e.g., X-ray photoelectron spectroscopy (XPS) in the investigation of adsorbed oxygen species and their effect on the catalytic activity of silver in oxidation reactions [16–18]. However, the binding of metal particles to the HOPG surface involves the problem of weak metal–support interaction. Metal nanoparticles on the atomically flat terraces of HOPG are highly mobile, and this eventually results in the agglomeration of the particles near step edges. Obviously, the higher the reaction temperature, the higher the rate of this process [11, 19, 20]. This problem can be remedied by intentionally generating defects on the smooth graphite surface by means of Ar^+ ion bombardment [11–15]. As metal nanoparticles are evaporated onto the defect-containing surface, they bind to surface defects, which prevent their motion on the surface and their sintering upon heating. Such samples are suitable for investigation of the catalytic properties of the material [16–18].

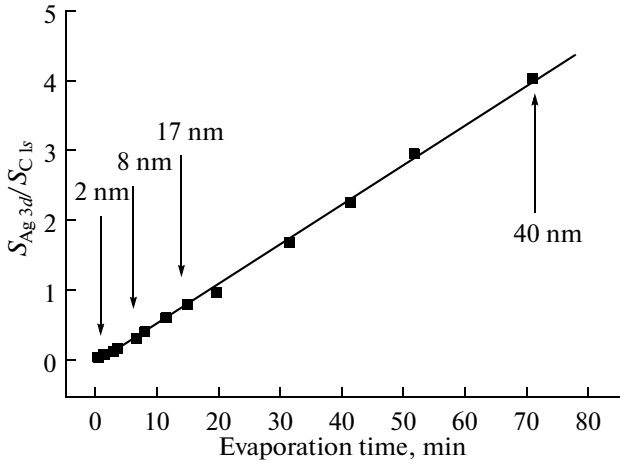

Fig. 1. Silver-to-carbon core level peak area ratio $S_{Ag\ 3d}/S_{C\ 1s}$ as a function of evaporation time. The mean diameter of Ag particles is indicated for some data points.

Here, we describe the preparation of Ag/HOPG catalysts with a narrow particle size distribution of the active component and report the catalyst particle size effect in ethylene oxidation.

EXPERIMENTAL

The preparation of Ag/HOPG samples and investigation of their thermal stability were carried out in vacuum chambers of an SPECS spectrometer fitted with a source of monochromated X-ray radiation (AlK_α, $h\nu = 1486.74$ eV) and a PHOIBOS-150-MCD-9 hemispherical analyzer. The sample preparation procedure included cleaning of the initial HOPG support (HOPG SPI-3, Structure Probe Inc.) and annealing of the support in a high vacuum at 500°C for 1 h. The purity of the surface was checked by recording a survey X-ray photoelectron spectrum and examining it for the presence of impurities. Defects on the HOPG surface were generated by soft Ar^+ ion bombardment (argon pressure of $P_{Ar} = 3.2 \times 10^{-6}$ mbar, accelerating voltage of 0.5 kV, bombardment time of 2–3 s).

Silver was evaporated by electron-impact heating of the target (99.95% Ag, Omicron EFM3 evaporation system) and was then deposited on a support maintained at room temperature at constant evaporation parameters (accelerating voltage of 0.8 kV, emission current of 3.5 mA). The metal concentration on the support surface was controlled by varying the evaporation time. The relative supported metal content was determined as the ratio of the areas of the silver and carbon core electron peaks (S_{Ag3d}/S_{C1s}) and was designated Ag/C. At fixed metal evaporation conditions, Ag/C increased linearly with time (Fig. 1). This made it possible to deposit a preset amount of metal accurate to a few tenths of a monolayer under high-vacuum conditions at room temperature. After Ag deposition, the samples were heat-treated at 300°C for stabilizing the nanoparticles on surface defects in order to prevent their agglomeration [21].

The samples were examined by scanning tunneling microscopy (STM) on a GPI-300.02 microscope, which allowed atomically resolved images of the conducting surface to be obtained at room temperature. The STM images were obtained using a platinum tip. Scanning was performed in the tunneling current range from 0.5 to 1 nA and in the voltage range from −30 to −1500 mV. Image processing included average slope subtraction and drift elimination using the WS×M software [22].

Catalytic properties were studied at the Innovative Station for In Situ Spectroscopy (ISISS beamline, BESSY II synchrotron radiation source, Berlin). A detailed description of the spectrometer is presented elsewhere [23, 24]. An important feature of this spectrometer is that it allows X-ray photoelectron spectra to be recorded at reaction mixture pressures of up to several millibars over the sample surface. The exciting radiation energy was set so that the initial kinetic energy of the photoelectrons was the same (220 eV) for all lines examined. The processing of the initial spectra included normalization of the photoelectron peak areas to the photoflux from the synchrotron radiation source with the spectral transfer function of the monochromator taken into account. Photoelectron line positions were corrected using the Fermi level as the reference.

Ethylene as a component of the product mixture was determined on a photon transfer reaction mass spectrometer (Ionicon Analytik, Austria) in which H^+ from the H_3O^+ ion is transferred to the ethylene oxide molecule (C_2H_4O) and the resulting $C_2H_5O^+$ ion is detected as $m/z = 45$ [25].

RESULTS AND DISCUSSION

Figure 2 shows the STM images and the corresponding particle size distributions for three samples prepared under identical conditions, but with silver particles deposited onto the support for different times. As the amount of evaporated metal is increased, the mean diameter (d_{mean}) of silver nanoparticles grows from 2 to 17 nm. The particles retain their spherical shape and are fairly uniformly distributed on the graphite surface. The procedure that we used to prepare the Ag/HOPG model catalysts makes it possible to obtain materials with the preset size of the metal nanoparticles, a sufficiently narrow particle size distribution, and stable under typical reaction temperatures (up to 250°C).

The size effect in ethylene oxidation was studied on two Ag/HOPG samples with different metal particle sizes. Figure 3 presents the STM images of silver nanoparticles supported on the defective HOPG surface and the corresponding particle size distributions for two samples differing in Ag/C ratio.

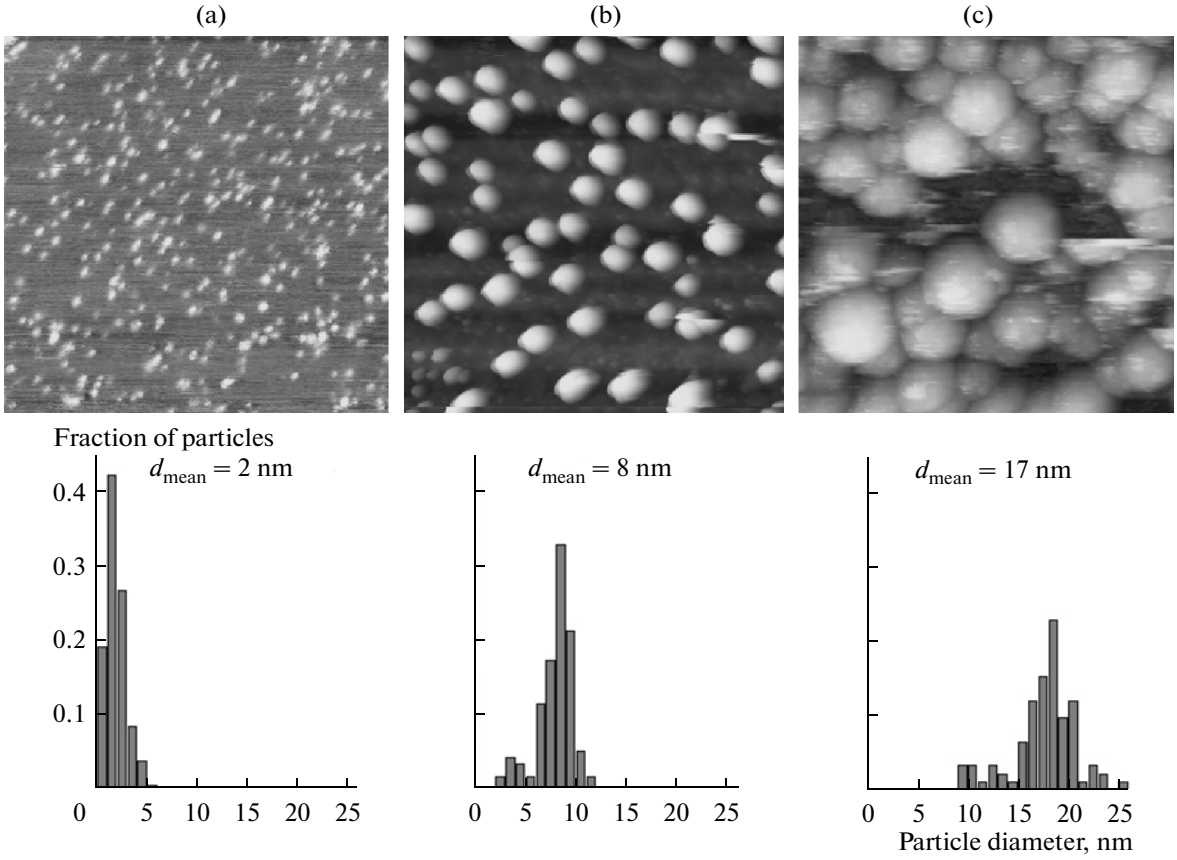

Fig. 2. STM images (100 × 100 nm) and silver particle size distribution for the defect-containing HOPG surface with Ag/C = (a) 0.13, (b) 0.40, and (c) 0.80. Imaging conditions: (a) $I = 0.5$ nA, $V = -1000$ mV; (b) $I = 0.5$ nA, $V = -1500$ mV; (c) $I = 1.0$ nA, $V = -1500$ mV.

The surface of the sample with Ag/C = 0.4 (Fig. 3a) is uniformly covered with separate silver particles, so the number of particles that are in contact with one another is small. The Ag nanoparticles are characterized by a rather narrow size distribution with d_{mean} = 8 nm (Fig. 3c). The surface of the sample richer in silver, with Ag/C = 4 (Fig. 3b), is almost entirely covered with metal particles being in close contact and showing distinct interparticle boundaries. As was expected, the particle size is distribution in this case is much wider and d_{mean} is about 40 nm (Fig. 3d).

The Ag/HOPG samples were tested in ethylene oxidation using in situ XPS. The reaction was conducted under the following conditions: ethylene : oxygen = 2 : 1, $P = 0.5$ mbar, 150–210°C. While recording X-ray photoelectron spectra, we simultaneously measured the ethylene oxide content of the reaction products by proton transfer reaction mass spectrometry [25]. The O 1*s* spectra and the corresponding ethylene oxide mass spectra recorded for these samples between 150 and 210°C are presented in Fig. 4. The O 1*s* spectra of both samples show several photoelectron lines (Figs. 4a, 4b). According to the literature, the high-energy region of the spectrum is the locus of the signals from oxygen groups located on the graphite surface: the signals at BE = 531.6–532.2 eV are due to the groups having a C=O bond (carbonyl, carboxyl, and ester groups), and the signals at BE > 533 eV are due to the groups having a C–O bond (hydroxyl, carboxyl, and ether groups) [26, 27]. The signals from the oxygen species adsorbed on the silver surface occur at lower energies (<531 eV) [7–10, 28, 29].

Under the reaction conditions, the silver particles with an mean diameter of about 8 nm mainly accommodate oxygen species characterized by O 1*s* BE = 530.8 ± 0.2 eV, and the intensity of the corresponding signal increases markedly as the reaction temperature is raised (Fig. 4a). The absence of the $m/z = 45$ line characteristic of ethylene oxide that the sample with small Ag particles is inactive in epoxidation (Fig. 4c).

The O 1*s* photoelectron spectrum of the sample with larger silver particles (d_{mean} = 40 nm, Ag/C = 4) in the reaction medium at 150°C shows two peaks due to oxygen species on the silver surface. These are the strong peak at 530.8 ± 0.2 eV and the peak at 529.2 ± 0.2 eV. Raising the temperature of the sample in the reaction medium to 210°C considerably strengthens the peak occurring at the lower binding energy. This indicates an increase in the concentration of oxygen adsorbed on silver. Heating the sample in the reaction

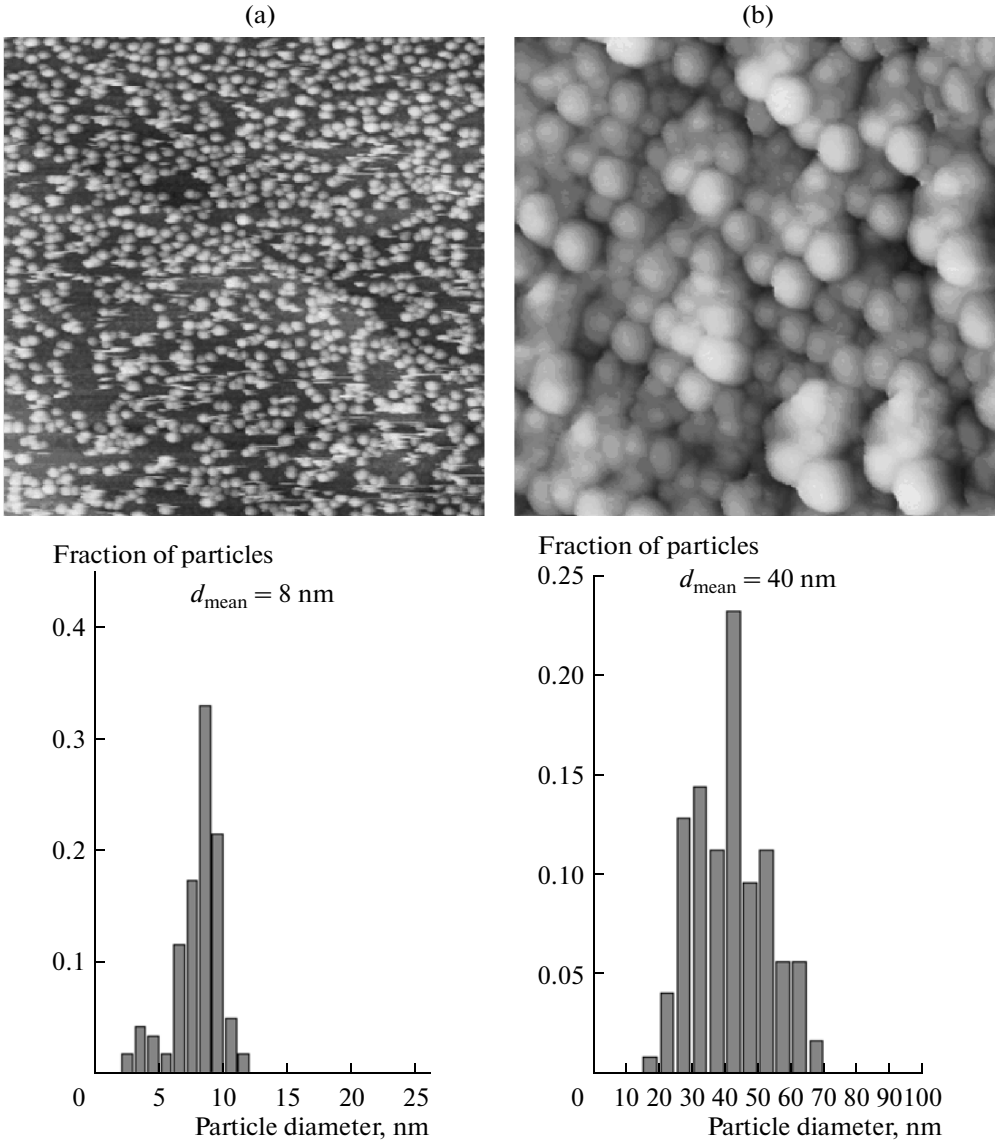

Fig. 3. STM images (500 × 500 nm) and particle size distribution for Ag/HOPG with Ag/C = (a, c) 0.4 and (b, d) 4. Imaging conditions: (a) $I = 1.0$ nA, $V = -30$ mV; (b) $I = 0.5$ nA, $V = -500$ mV.

medium is accompanied by the strengthening of the $m/z = 45$ mass spectrometric line, which is characteristic of the protonated ethylene oxide molecule (Fig. 4d). The sharp increase in the intensity of this line at the 30th minute is likely a consequence of the intensive evolution of ethylene oxide from adsorbed complexes that are stable on the silver surface below 165°C. After that, ethylene oxide formation comes to a steady-state level. Because the experiments were performed at a low reactant pressure (0.5 mbar) and the ethylene oxide formation rate was very low, the performance characteristics of the mass spectrometer did not allow us to estimate the ethylene oxide concentration quantitatively and then calculate the ethylene oxide selectivity. In addition, in view of the low concentration of the total oxidation products (CO_2 and H_2O), it was impossible to use the signal from the quadrupole mass spectrometer in quantitative calculations.

There has been an XPS study of oxygen adsorption on Ag/C model systems prepared by thermal evaporation of silver onto amorphous carbon [30, 31]. The surface area of evaporated silver covered by the two types of adsorbed oxygen species was found to depend on the silver concentration, which was estimated as the ratio of the integrated intensities of the Ag 3*d* and C 1*s* peaks ($I_{Ag\,3d}/I_{C\,1s}$). For example, the O_2 treatment of Ag/C with $I_{Ag\,3d}/I_{C\,1s} < 10$ ($P = 0.1$ mbar, $T = 200$°C) yields only the electrophilic species of adsorbed oxygen. Raising $I_{Ag\,3d}/I_{C\,1s}$ to 15 or above leads to the appearance of the nucleophilic species. The authors of those studies hypothesized that the corresponding spectral changes are to the increase in the mean size of

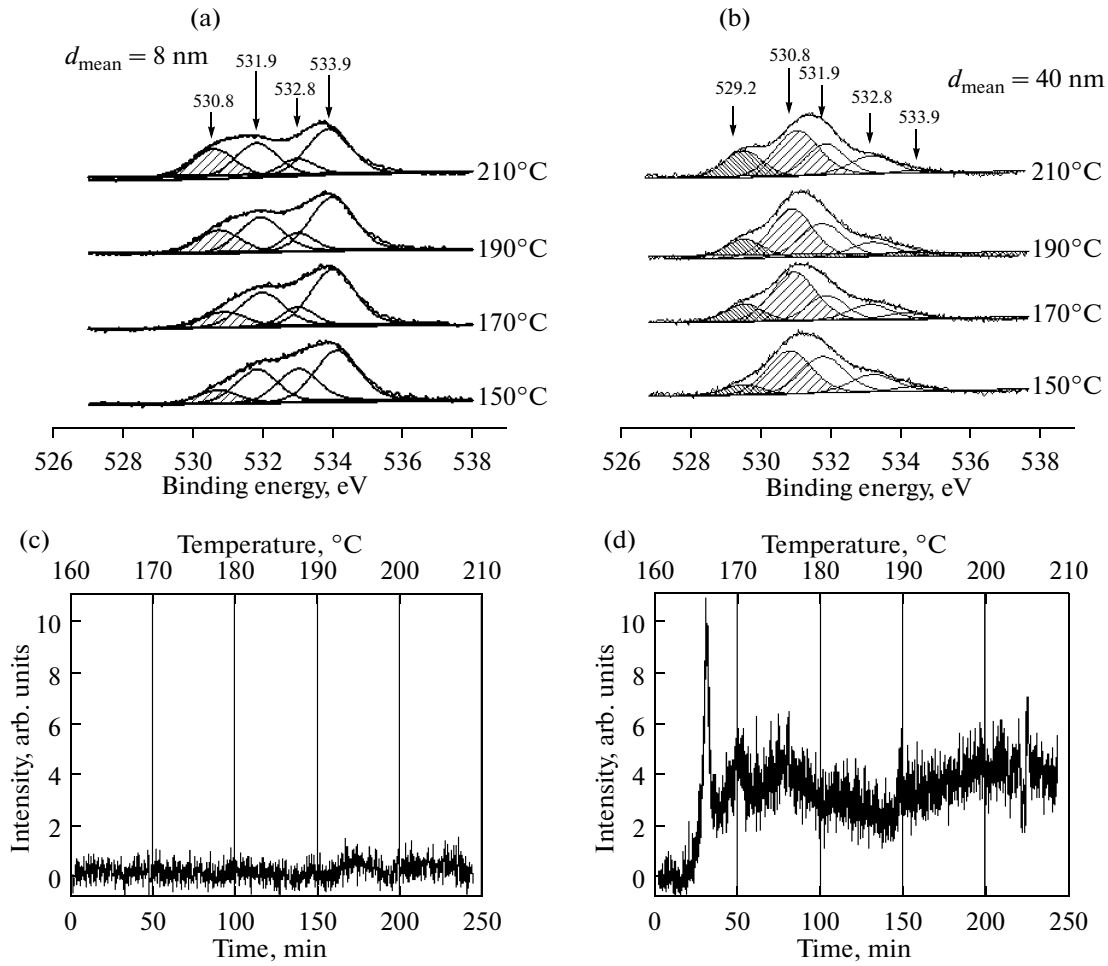

Fig. 4. O 1*s* photoelectron spectra of Ag/HOPG samples with Ag/C = (a) 0.4 and (b) 4 and (c, d) *m/z* line intensity in the mass spectrum of ethylene oxide forming on these samples as a function of temperature and reaction time. Experimental conditions: $C_2H_4 : O_2 = 2 : 1$, $P = 0.5$ mbar. The mean Ag particle size is indicated on panels (a) and (b). The signals from the oxygen species adsorbed on silver are hatched.

the silver particles; however, no direct experimental evidence of the formation of three-dimensional supported silver particles was presented. Thus, the authors were unable to correlate the concentration of deposited silver with the mean size of the silver particles.

Our data for the catalyst in the oxygen–ethylene reaction mixture are not in conflict with the basic conclusions made in the above-cited works as to the effect of the silver concentration on the formation of adsorbed oxygen species. At the same time, our data make it possible to correlate the observed changes in the nature of the adsorbed species to the Ag particle size. The main oxygen species forming on small silver particles (d_{mean} = 8 nm) is that characterized by BE = 530.8 ± 0.2 eV, and, according to the literature, this species can be identified both as O_{el} atoms adsorbed on the silver surface [29, 32] and as oxygen dissolved in the subsurface layers of the metal [29, 33]. The formation of surface carbonates, whose O 1*s* binding energy has a similar value (~530.5 eV), can be excluded from consideration because their decomposition temperature is below 150°C [1, 34]. The oxygen species forming under the reaction conditions on larger silver particles is that characterized by BE = 529.2 ± 0.2 eV, which can be identified as nucleophilic oxygen, and that characterized by BE = 530.8 ± 0.2 eV. The assumption that the latter O 1*s* signal is partly due to oxygen dissolved in the subsurface layers of silver is verified by experimental data on the depth distribution of oxygen species in Ag particles (Fig. 5). Clearly, as the probing depth is increased by raising the kinetic energy of the emitted photoelectrons by using higher energy incident X-ray photons, the intensity ratio of the O 1*s* signal at 529.2 to the O 1*s* signal at 530.8 eV decreases. Therefore, the oxygen species characterized by BE = 529.2 eV is more "surface-located" than the species characterized by BE = 530.8 eV. In other words, at least part of the O 1*s* signal at 530.8 eV is due to the oxygen dissolved in the subsurface layers of silver [29, 33].

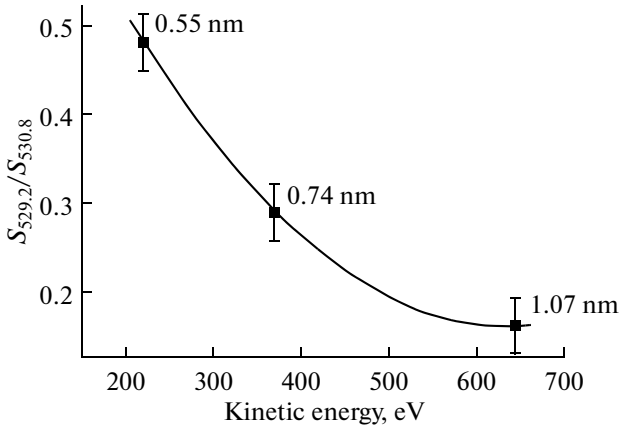

Fig. 5. Ratio of the BE = 529.2 and 530.8 eV O 1*s* peak areas as a function of the kinetic energy of emitted photoelectrons for Ag/HOPG with $d_{mean} = 40$ nm. The photoelectron mean free path (probing depth) calculated via the formula presented in [35] is indicated for each data point. Spectrum acquisition conditions: $C_2H_4 : O_2 = 2 : 1$, $T =$ 210°C, $P = 0.5$ mbar.

The presence of adsorbed oxygen species with BE = 529.2 and 530.8 eV on the silver surface is the key factor in ethylene oxide formation on the Ag/HOPG model catalysts. On the one hand, the low ethylene epoxidation activity of the sample with the low silver coverage of the surface (Ag/C = 0.4) can be explained by the fact that it has a lower surface concentration of active sites than the Ag/C = 4 sample. On the other hand, it is more likely that the former sample is inactive because it has no nucleophilic oxygen. Accordingly, the activity of the sample with larger Ag particles is most likely due to the higher concentration of nucleophilic oxygen on its surface, implying an increase in the adsorbed ethylene coverage of the silver surface [6].

Thus, thermal evaporation of silver on defect-containing HOPG surface provides a means to obtain model catalysts with a narrow and variable particle size distribution in the nanometer range. The resulting catalysts are sintering-resistant at temperatures typical of ethylene oxidation.

Use of the Ag/HOPG model systems makes it possible to differentiate between oxygen species adsorbed on the silver and graphite surfaces in terms of their O 1*s* binding energies in the X-ray photoelectron spectrum. This makes the Ag/HOPG catalysts helpful in the in situ XPS investigation of the surface of silver nanoparticles in catalytic ethylene oxidation.

In this study, Ag/HOPG catalysts with different Ag particle sizes we tested for the first time in ethylene epoxidation using in situ XPS. The most abundant oxygen species forming on silver particles ~8 nm in diameter in the C_2H_4/O_2 reaction mixture ($P = 0.5$ mbar) is electrophilic oxygen, which, together with oxygen dissolved in the subsurface layers of silver, gives rise to an O 1*s* signal at BE = 530.8 ± 0.2 eV. On larger silver particles 30–50 nm in diameter, the formation of nucleophilic oxygen species also takes place, which is indicated by the appearance of an O 1*s* signal at 592.2 ± 0.2 eV. It is the presence of both adsorbed oxygen species (O_{nucl} and O_{el}) that makes the sample with larger silver particles active in ethylene oxide formation.

ACKNOWLEDGMENTS

This work was supported by the Siberian Branch of the Russian Academy of Sciences (Interdisciplinary Projects Program, project no. 9).

REFERENCES

1. *Supported Metals in Catalysis,* Anderson, J.A. and Garcia, M.F., Eds., London: Imperial College Press, 2005.
2. Che, M. and Bennett, C.O., *Adv. Catal.*, 1989, vol. 36, p. 55.
3. De Oliveira, A.L., Wolf, A., and Schüth, F., *Catal. Lett.*, 2001, vol. 73, p. 157.
4. Lei, Y., Mehmood, F., Lee, S., Greeley, J., Lee, B., Seifert, S., Winans, R.E., Elam, J.W., Meyer, R.J., Redfern, P.C., Teschner, D., Schlögl, R., Pellin, M.J., Curtiss, L.A., and Vajda, S., *Science*, 2010, vol. 328, p. 224.
5. Verykios, X.E., Stein, F.P., and Couglin, R.W., *J. Catal.*, 1980, vol. 66, p. 368.
6. Goncharova, S.N., Paukshtis, E.A., and Bal'zhinimaev, B.S., *Appl. Catal., A*, 1995, vol. 126, p. 67.
7. Grant, R.B. and Lambert, R.M., *J. Catal.,* 1984, vol. 92, p. 364.
8. Bukhtiyarov, V.I., Boronin, A.I., and Savchenko, V.I., *J. Catal.*, 1994, vol. 150, p. 262.
9. Bukhtiyarov, V.I., Prosvirin, I.P., and Kvon, R.I., *Surf. Sci.*, 1994, vol. 320, p. L47.
10. Bukhtiyarov, V.I., Kaichev, V.V., Podgornov, E.A., and Prosvirin, I.P., *Catal. Lett.*, 1999, vol. 57, p. 233.
11. Lopez-Salido, I., Lim, D.C., and Kim, Y.D., *Surf. Sci.*, 2005, vol. 588, p. 6.
12. Stable, A., Eichhorst-Gerner, K., Rabe, J.P., and Gonzalez-Elipe, A.R., *Langmuir*, 1998, vol. 14, p. 7324.
13. Palmer, R.E., Pratontep, S., and Boyen, H.-G., *Nat. Mater.*, 2003, vol. 2, p. 443.
14. Hövel, H., Becker, Th., Bettac, A., Reihl, B., Tschudy, M., and Williams, E.J., *J. Appl. Phys.,* 1997, vol. 81, p. 154.
15. Wang, L.L., Ma, X.C., Qi, Y., Jiang, P., Jia, J.F., Xue, Q.K., Jiao, J., and Bao, X.H., *Ultramicroscopy,* 2005, vol. 105, p. 1.
16. Lim, D.C., Lopez-Salido, I., Dietsche, R., Bubek, M., and Kim, Y.D., *Surf. Sci.,* 2006, vol. 600, p. 507.
17. Carley, A.F., Dollard, L.A., Norman, P.R., Pattage, C., and Roberts, M.W., *J. Electron Spectrosc. Relat. Phenom.,* 1999, vols. 98–99, p. 223.
18. Lim, D.C., Lopez-Salido, I., and Kim, Y.D., *Surf. Sci.*, 2005, vol. 598, p. 96.

19. Kholmanov, I.N., Gavioli, L., Fanetti, M., Casella, M., Cepek, C., Mattevi, C., and Sancrotti, M., *Surf. Sci.*, 2007, vol. 601, p. 188.

20. Walter, E., Murray, B., Favier, F., Kaltenpoth, G., Grunze, M., and Penner, R., *J. Phys. Chem. B*, 2002, vol. 106, p. 11407.

21. Demidov, D.V., Prosvirin, I.P., Sorokin, A.M., and Bukhtiyarov, V.I., *4-ya shkola "Metrologiya i standartizatsiya v nanotekhnologiyakh i nanoindustrii: Funktsional'nye nanomaterialy"* ("Metrology and Standardization in Nanotechnologies and Nano Industry: Functional Materials," Proc. 4th Workshop), Novosibirsk, 2011, p. 69.

22. Horcas, I., Fernandez, R., Gomez-Rodriguez, J.M., Colchero, J., Gomez-Herrero, J., and Baro, A.M., *Rev. Sci. Instrum.*, 2007, vol. 78, p. 013705-1.

23. Knop-Gericke, A., Kleimenov, E., Hävecker, M., Blume, R., Teschner, D., Zafeiratos, S., Schlögl, R., Bukhtiyarov, V.I., Nizovskii, A., Bluhm, H., Barinov, A., Dudin, P., and Kiskinova, M., *Adv. Catal.,* 2009, vol. 52, p. 213.

24. Bluhm, H., Hävecker, M., Knop-Gericke, A., Kiskinove, M., Schlögl, R., and Salmeron, M., *MRS Bull.*, 2007, vol. 32, p. 1022.

25. Lindinger, W., Hansel, A., and Jordan, A., *Chem. Soc. Rev.,* 1998, vol. 27, p. 347.

26. Kundu, S., Wang, Y., Xia, W., and Muhler, M., *J. Phys. Chem. C*, 2008, vol. 112, p. 16869.

27. Langle, L.A., Villanueva, D.E., and Fairbrother, D.H., *Chem. Mater.*, 2006, vol. 18, p. 169.

28. Bukhtiyarov, V.I., Nizovskii, A.I., Bluhm, H., Hävecker, M., Kleimenov, E., Knop-Gericke, A., and Schlögl, R., *J. Catal.*, 2006, vol. 238, p. 260.

29. Bao, X., Muhler, M., Schedel-Neidrig, Th., and Schlögl, R., *Phys. Rev. B: Condens. Matter*, 1996, vol. 54, p. 2249.

30. Bukhtiyarov, V.I., Carley, A.F., Dollar, L.A., and Roberts, M.W., *Surf. Sci. Lett.*, 1997, vol. 381, p. L605.

31. Bukhtiyarov, V.I. and Kaichev, V.V., *J. Mol. Catal. A: Chem.*, 2000, vol. 158, p. 167.

32. Bukhtiyarov, V.I., Boronin, A.I., Prosvirin, I.P., and Savchenko, V.I., *J. Catal.*, 1994, vol. 150, p. 268.

33. Waterhouse, G.I.N., Bowmaker, G.A., and Metson, J.B., *Appl. Catal., A*, 2004, vol. 265, p. 85.

34. Salaita, G.N., Hazos, Z.F., and Hoflund, G.B., *J. Electron Spectrosc. Relat. Phenom.*, 2000, vol. 107, p. 73.

35. Tanuma, S., Powell, C.J., and Penn, D.R., *Surf. Interface Anal.*, 1993, vol. 21, p. 165.